

Production of spin-polarized electrons by photoemission from GaAs(110)

B. Reihl, M. Erbudak, and D. M. Campbell*

Laboratorium für Festkörperphysik, Eidgenössische Technische Hochschule, 8093 Zürich, Switzerland

(Received 25 January 1979)

The properties of the spin-polarized electron source based on photoemission from Zn-doped GaAs depend on the degree of surface coverage with cesium and oxygen. In the case of a negative-electron-affinity surface a systematic depolarization of the emitted electrons takes place by exchange scattering in the Cs-O overlayer. It is deduced from the temperature dependence of the spin polarization that electrons which have for $h\nu > 1.8$ eV thermalized into the L valley are less depolarized in the overlayer as well as in the bulk than the electrons which stem from the Γ point. Accordingly we suggest that the L -point electrons be used in a source of polarized electrons, and present our specific and simple design.

I. INTRODUCTION

Spin-polarized electron beams are being used increasingly in experiments in solid-state physics, atomic physics, and high-energy physics.¹⁻⁵ This is mainly due to the recent development of efficient sources of spin-polarized electrons. In 1974 it was suggested by Garwin, Pierce, and Siegmann⁶ that photoemission induced by irradiation of a Cs and O₂ treated GaAs surface with circularly polarized light could provide an intense source of electrons with polarization (P) up to 0.5. Pierce *et al.*⁷ confirmed the qualities of GaAs as a source, although it became clear that the cleaning of the GaAs surface and its subsequent Cs and O₂ coverage necessary to obtain a high photoelectric yield (Y) influenced the electron spin polarization (ESP). Since that time the construction of GaAs sources has been undertaken in several laboratories, and different methods are being used to achieve the proper surface treatment. First results show that the promise of the original investigations⁷ must be qualified by the realization that highest P and highest Y exclude each other.⁸

Here we report on the development of a GaAs source which is now in use in the study of spin-dependent phenomena in low-energy electron diffraction (LEED). Two features of the source offer particular practical advantages: (i) the GaAs crystal is cleaved *in vacuo*, thus eliminating the necessity for elaborate cleaning and annealing of the cathode; (ii) the creation of a positive electron affinity (PEA) surface yields a maximum polarization $P=0.35$ for a photon energy near $h\nu=1.96$ eV, allowing high currents to be generated using an inexpensive He-Ne laser as the light source.

II. THEORETICAL CONSIDERATIONS

The ESP is nonrelativistically defined as²

$$\vec{P} = \text{Tr} \vec{\sigma} \rho, \quad (1)$$

where $\vec{\sigma}$ is the Pauli spin matrix vector and ρ is the spin-state density matrix. In the present case it is sufficient to define the degree of polarization as the normalized difference of the number of electrons having their spins parallel ($n\uparrow$) and anti-parallel ($n\downarrow$) to the axis of quantization defined by the angular momentum of the circularly polarized light⁷:

$$P = (n\uparrow - n\downarrow)/(n\uparrow + n\downarrow). \quad (2)$$

Arbitrarily we call \vec{P} positive for irradiation with σ_+ circularly polarized light (light angular momentum in light propagation direction).

In direct band-gap III-V compounds the initial ESP, i.e., directly after photoexcitation, has up to now been found to be highest for $h\nu = E_G$ (E_G : band-gap energy). The optical transitions are from the spin-orbit split p -like valence band to the s -like conduction band. Near the Γ -point ($k=0$) the transition probabilities allow one spin direction of the photoexcited electrons to be three times as much populated as the other, resulting in a theoretical initial polarization $P_i = (3-1)/(3+1) = 0.50$.⁹ For higher photon energies ($k>0$) emission from the split-off part of the valence band sets in at $h\nu = E_G + \Delta$, and decreases P_i to zero.

Several relaxation processes¹⁰ diminish the ESP of the conduction electrons before their escape into vacuum. Thus the essential bulk polarization P_L , monitored by measuring the polarization of the recombination luminescence,¹⁰ is lower than P_i . To extract the conduction-band electrons into vacuum it is necessary to lower the vacuum level close to the conduction band edge. The highest Y and therewith a desirable high intensity of spin polarized electrons is in fact obtained if the vacuum level is reduced below the Γ -point minimum.¹¹ This unique case of negative electron affinity (NEA) may be achieved by appropriate cesium and oxygen deposition, and is clearly recognizable by the rectangular Y curve [cf. Fig. 1(a)]; there is,

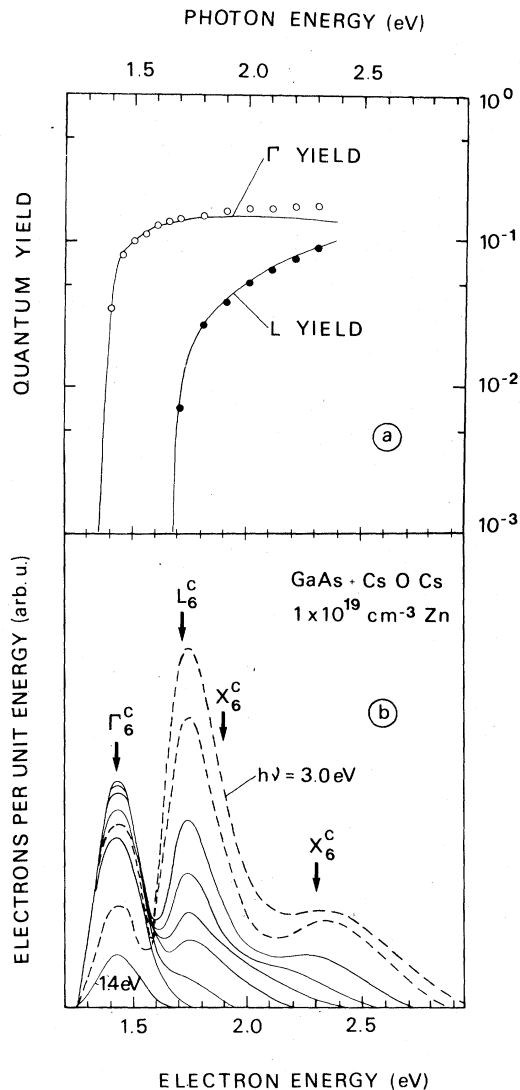


FIG. 1. (a) Quantum yield as function of photon energy in eV for electrons originating from the Γ -point valley (Γ yield) and the L -point valley (L yield). The solid line represents theory, the points are experimental (after James and Moll, Ref. 12). (b) Normalized and smoothed experimental energy distribution curves for a photon energy of 1.4–3.0 eV in increments of 0.2 eV (after James and Moll, Ref. 12, with the reinterpretation by Aspnes, Ref. 13). Electron energies are given relative to the top of the valence band. Clearly visible is the emission of only two groups of electrons, namely, at Γ and L .

on the other hand, an infinite number of PEA cases, each with a different phototreshold [cf., e.g., Fig. 1(a)]. A further depolarization can take place due to spin exchange scattering when the electrons pass through the Cs-O layer.⁸ Classifying all this in the three step process of photoemission,¹¹ (a) optical absorption, (b) transport to the surface,

and (c) escape across the surface into vacuum, one finds for our measured P

$$P_i \xrightarrow[\text{(a)}]{\text{spin relaxation}} P_L \xrightarrow[\text{(b)}]{\text{exchange scattering}} P \xrightarrow[\text{(c)}]{\text{escape}} P. \quad (3)$$

From energy distribution measurements on photoelectrons from heavily Zn-doped GaAs with a Cs-O-Cs layer,¹² it is known [cf. Fig. 1(b)] that in the photon energy range $1.4 < h\nu < 3.0$ eV only two groups of electrons are emitted: the one located at an energy of 1.43 eV stems from excited electrons which have thermalized into the Γ -point valley ($h\nu < 1.8$ eV), the other at 1.75 eV is interpreted¹³ as being due to electrons which have thermalized into the L -point valley ($h\nu > 1.8$ eV). The electrons escape into vacuum with a kinetic energy of 0.2 and 0.5 eV, respectively.

III. EXPERIMENTAL LAYOUT

A. Source

A schematic diagram of the source is shown in Fig. 2. The GaAs crystal (2) is mounted in a sapphire holder, which is attached to the base of a cold trap, allowing the crystal to be cooled to 80 K while maintaining electrical isolation. A bellows permits the cold trap with the crystal to be raised 10 mm for cleavage (1) and cesiation (8). It also allows the position of the cathode to be adjusted to optimize the electron optical properties of the extraction lenses, consisting of a Wehnelt-type diaphragm (3) and accelerating anode (4). These together with the steering plates (5), the spherical deflectors (6), and the cesium dispenser (8)¹⁴ are attached by glass insulators to a structure mounted on the upper 4" flange of the vacuum chamber. The cleavage tool (1) operated by a linear motion drive is mounted on a side port.

All electrodes are of nonmagnetic stainless steel; the spherical deflector plates (6) are sections cut from two spherical shells, 1 mm thick with internal radii of 40 and 60 mm. A small hole cut in the larger plate allows the cathode to be illuminated by either the linearly polarized light from a 10-mW He-Ne laser or the monochromized light from a Xe lamp (13)–(15) followed by a linear polarizer (12).¹⁵ A mechanically rotated retarder (11)¹⁶ is used to change the polarization of the light from linear to right or left circular. The electron beam deflection system is followed by a four cylinder zoom lens (cf. Fig. 3), the first element incorporating an uhv straight-through valve. The whole system is pumped to a base pressure of 5×10^{-11} Torr by a 100 l/s ion pump (16). During the experiment a nitrogen-cooled titanium pump

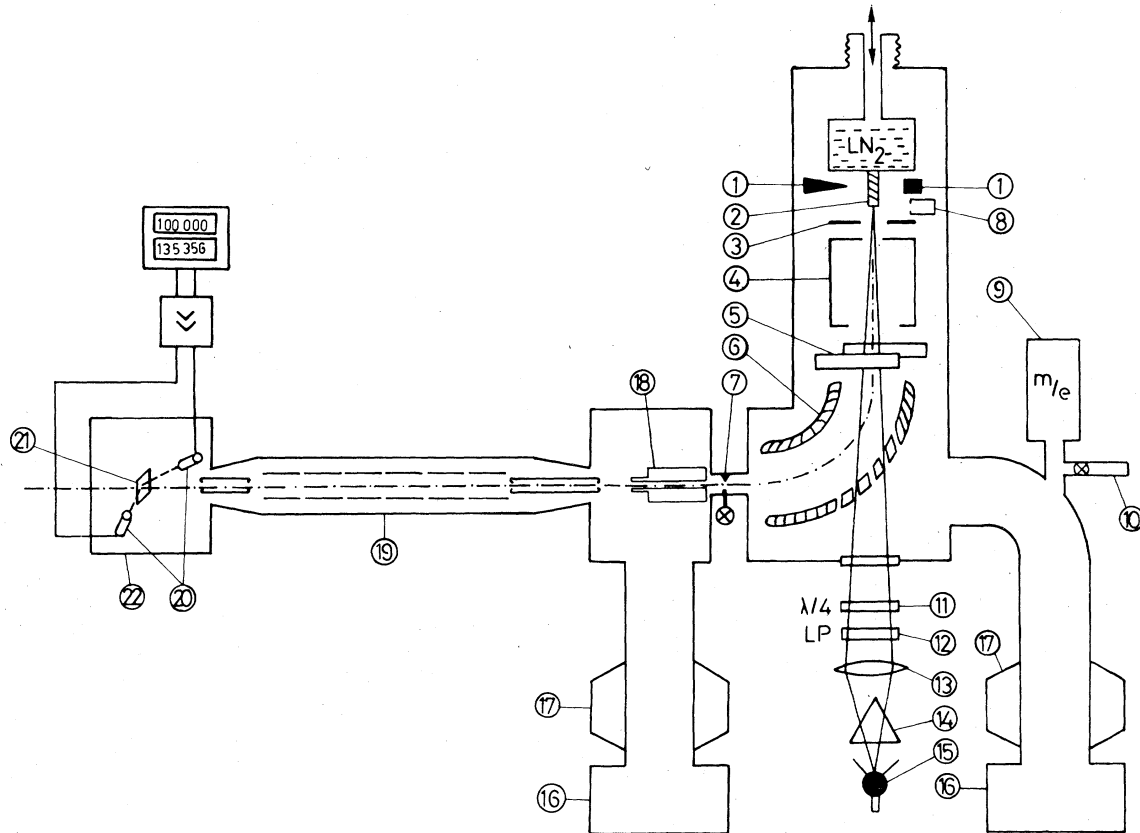


FIG. 2. Schematic diagram of the apparatus: (1) cleaver, (2) GaAs crystal, (3) diaphragm, (4) anode, (5) deflection plates, (6) spherical condenser, (7) vacuum interlock, (8) cesium dispenser, (9) mass spectrometer, (10) oxygen source, (11) retarder, (12) linear polarizer, (13)–(15) monochromatic light, (16) ion pump, (17) LN₂ and titanium pump, (18) field lens system, (19) 100 kV accelerator, (20) detectors at ±120°, (21) gold foil, and (22) Mott chamber.

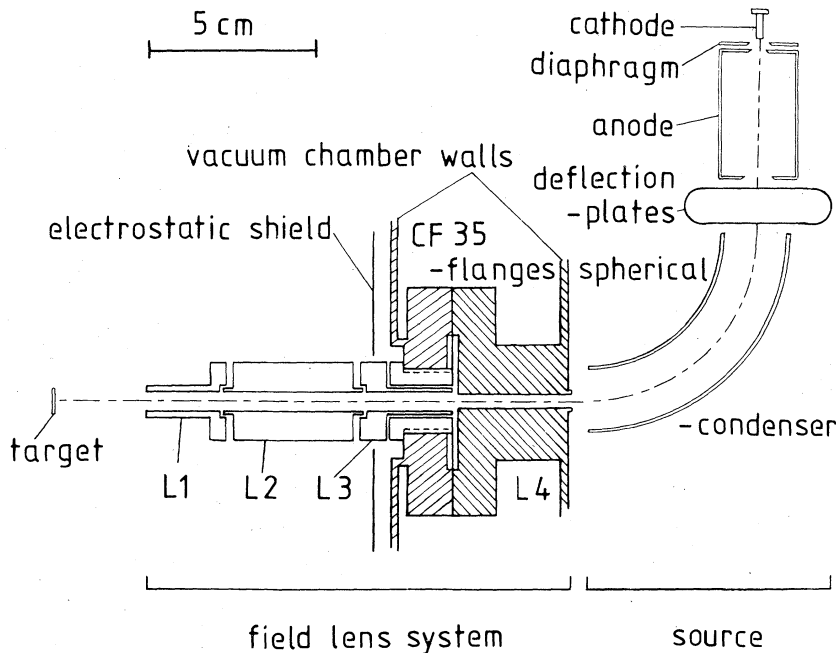


FIG. 3. Scale drawing of the electron optics. Note that L4 incorporates an uhv valve which is not shown for clarity. The supporting parts of the field lens system are also omitted. The kinetic energy of the electrons is given by the voltage V_1 applied to L1. Target and electrostatic shield are also on V_1 potential.

(17) is also used to reduce the condensation of residual gases on the cooled cathode. Oxygen (to maximum 10^{-8} Torr) enters the system through a heated silver tube (10) which can be locked off by a needle valve.

B. Electron optics

Photoelectrons liberated when the cathode is illuminated by circularly polarized light are polarized along the direction of the incident light beam.⁷ A two aperture extraction lens accelerates the electron beam to 400 eV, at which energy it passes through a pair of steering plates into a spherical deflector. The latter rotates the momentum vector through 90° without influencing the polarization vector, and thereby converts longitudinal into transverse polarization, necessary to study either spin-orbit coupling effects in LEED⁴ or to determine the ESP by Mott scattering (cf. Sec. III D). The two-dimensional focusing property of the spherical condenser¹⁷ is used to converge the beam to give an image of the cathode at the effective entrance aperture of the zoom lens, within the uhv valve. A scale drawing of the electron optics is shown in Fig. 3.

The zoom lens is based on the field lens design of Kurepa *et al.*¹⁸ using four cylinders long enough to constitute three effectively independent lenses. The first lens decelerates the electrons to 50 eV and images the entrance aperture on the first principal plane of the second lens. Since the positions of the principal planes of a two-cylinder lens are almost independent of voltage ratios in the range of 3–30,¹⁹ the second lens is used to accelerate the beam to between 120 and 1200 eV, while giving a fixed image of approximately unit magnification close to the second principal plane. This image then becomes the object for the third lens, which decelerates the beam with a fixed ratio of 1/3.5 to give an image at the target. The overall magnification of the zoom lens is +3 and is independent of the final beam energy.

C. Cathode preparation

Single crystals of degenerate *p*-doped GaAs²⁰ are cut into bars $2 \times 2 \times 10$ mm, with the axis perpendicular to the (110) cleavage plane. The Zn doping is normally 1×10^{19} cm⁻³, although samples with a higher doping of 5×10^{19} cm⁻³ have also been used. A series of transverse grooves 1 mm apart are scribed on the side of the bar to facilitate the propagation of the cleavage tension *in vacuo*. Mechanical stress is removed by etching the crystal in a solution of 70% H₂O₂ + 30% H₂SO₄. The piece is then inserted into the crystal holder which is brought to its position (2) (cf. Fig. 2) through a side port.

When the light has properly been focused on the GaAs surface, a 1-mm segment is cleaved from the end of the crystal. The work function of the surface is then lowered in the standard way¹¹ by deposition of cesium from a dispenser.¹⁴ The reduction in work function is monitored by observation of the current emitted from the cathode, when illuminated by light with $h\nu = 1.5$ eV. Cesium is stopped when maximum photocurrent is attained, and oxygen is admitted into the system at a pressure of 10^{-8} Torr. When the photocurrent has dropped to 50% of its maximum value, the oxygen is shut off and the photocurrent maximized by further cesiation. An increase of the photocurrent with oxygen exposure is an indication that "over"-cesiation has occurred, i.e., the photocurrent has already been reduced by an excess of cesium.²¹ Simultaneous cesiation and oxygenation, the relative proportions being continuously adjusted to maximize the rate of increase of photocurrent, has not shown any practical advantage over the method described above. It is, however, essential for the creation of a stable surface that the cesium be deposited at as low a rate as practicable. The surface preparation takes about half an hour and is carried out at room temperature to ensure a uniform coverage. The crystal is then cooled to 83 ± 5 K at a rate of 13 K/h. This was checked in a separate run with a thermocouple connected to the crystal holder.

D. Spin detection

Measurement of the ESP is done by 100 kV Mott scattering from a gold foil target.²² It makes use of the spin-orbit coupling in back scattering of electrons from a high-*Z* material to determine the polarization component perpendicular to the scattering plane from the counting rates of two surface barrier detectors²³ located at polar angles of $\theta = \pm 120^\circ$. Five interchangeable foils²⁴ of different thickness are employed so that the reciprocal scattering asymmetry can be extrapolated to zero foil thickness, in order to eliminate the influence of multiple scattering within the gold foil. This procedure requires only knowledge of the relative foil thickness, which is obtained by comparing the count rates of foil-scattered electrons at constant primary beam intensity. In normal operation a foil with an effective analyzing power of $S_{\text{eff}} = 0.3$, calibrated by the above procedure, is used.

The Mott chamber is pumped through the six-stage accelerator by ion and titanium pumps to 6×10^{-9} Torr. The entire data acquisition system is operated at 100 kV. The pulses from the surface barrier detectors are amplified, discriminated in order to count only the elastically scattered electrons, and fed to counters operated in a mast-

er-slave mode (i.e., when a prechosen value is reached by the master counter, the slave counter and a clock are stopped). From the count rates P and Y are determined.

The experimental detector asymmetry is eliminated in two ways:

(i) Unpolarized electrons, obtained by using unpolarized or linearly polarized light, are scattered from the gold target. This gives an experimentally determined count rate ratio A . If Q_{\pm} is the count rate ratio in scattering of polarized electrons obtained by using σ_{\pm} polarized light, the true polarization is given by

$$P_{\pm} = \frac{1}{S_{\text{eff}}} \frac{Q_{\pm} - A}{Q_{\pm} + A}. \quad (4)$$

(ii) Scattering of polarized electrons from the gold target and reversing the spin-polarization vector by changing the light from σ_+ to σ_- gives

$$P = \frac{1}{S_{\text{eff}}} \frac{\sqrt{Q_+} - \sqrt{Q_-}}{\sqrt{Q_+} + \sqrt{Q_-}}. \quad (5)$$

Since the present source has the particular advantage that the beam properties are not changed by reversal of the polarization vector (in contrast with the case when the electrons are extracted from magnetic systems), method (ii) is normally used. Generally (i) and (ii) give the same results in our experiment, but (ii) is mostly used, as it eliminates the experimental asymmetry in every run, whereas (i) is used to bring A close to 1 by electron optical steering.

IV. RESULTS AND DISCUSSION

A. NEA GaAs

The creation of a NEA surface by the procedure described above is verified [cf. Fig. 1(a)] by measuring the quantum yield as a function of $h\nu$ using the Xe lamp with monochromator. In Fig. 4 typical results for NEA are presented both for 300 and 80 K. The Y curves exhibit a threshold below 1.4 eV and the characteristic "knee" around 1.5 eV (typical band-gap energy). Also shown are the ESP curves. The main effect of the temperature is that P increases by a factor of 1.2 to 1.3 in cooling from 300 to 80 K. In both cases the maximum P is at $h\nu = 1.55$ eV with a characteristic decrease towards lower light energies, which we attribute to emission either from impurities into the empty conduction band²⁵ or from the valence band into an empty surface state band.²⁶

For $h\nu > 1.55$ eV P smoothly drops towards higher photon energies as one goes away from Γ -point transitions. But clearly observable as a shoulder at $h\nu = 1.8$ eV is the onset of L -point emission, indicated by an arrow in Fig. 4 [see also Sec. II

and Fig. 1(b)]. In this context it has to be noted that we measure an integral ESP, i.e., the P of all electrons emitted at a given $h\nu$. In particular this means that possible structures in the P curve are smeared out. In the decreasing shoulder ($h\nu > 1.55$ eV) of Fig. 4 the L -point emission must, however, be more highly polarized in order to produce the observed structure. It is therefore desirable to discriminate in favor of this part of the P spectrum; it is shown below that this highly polarized L -point emission, which was not

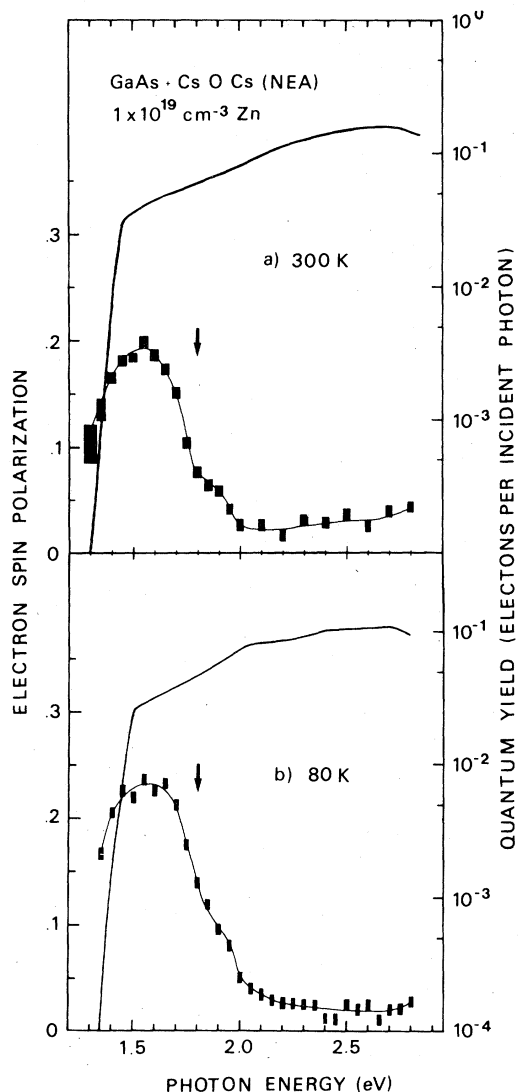


FIG. 4. Electron spin polarization (left ordinate, vertical extensions are twice the standard deviation of the Mott uncertainty, horizontal extensions give the resolution of the monochromator) and yield (continuous curve, right ordinate) from NEA GaAs at (a) 300 K and (b) 80 K. The arrows indicate the onset of L -point emission at $h\nu = 1.8$ eV.

observed up to now, is crucial for the easy production of spin-polarized electrons. On the other hand, the L -point peak is more pronounced in Fig. 4(a) (300 K) than in the 80 K spectrum [Fig. 4(b)] and exhibits about the same overall polarization. Clearly in a less polarized background [Fig. 4(a)] the onset of a more highly polarized electron emission is more pronounced. This also indicates that the L -point emission is much less affected than the Γ -point emission by spin relaxation processes responsible for the bulk depolarization [denoted as P_i to P_L in Eq. (3)]. Fishman and Lampel¹⁰ in a detailed discussion show that the only effective process in question is the exchange interaction between electrons and holes, as first proposed by Bir, Aronov, and Pikus,²⁷ at least for temperatures $T < 100$ K. At room temperature the picture is not so clear,¹⁰ but spin relaxation by scattering from impurities or phonons could be dominant. An increase of the bulk depolarization is already found in the luminescence polarization P_L in going from 1 to 100 K.¹⁰

By interpolation for 80 K and our doping of $1 \times 10^{19} \text{ cm}^{-3}$ Zn, we find $P_L (h\nu = 1.6 \text{ eV}) = 0.30$ from Figs. 2 and 5 of Ref. 10. This value compares with our $P_{\text{max}} = 0.23$ of Fig. 4(b). The further depolarization is attributed to exchange scattering in the Cs-O-Cs overlayer,⁸ which the Γ -point electrons traverse with a kinetic energy of 0.2 eV. With the strongly energy dependent exchange cross section²⁸ of alkalis it was possible to show⁸ that preponderantly Cs_2O with no free electron spins is formed, but some physisorbed Cs atoms of the second coverage act as spin scatterers. On the other hand it is not exactly known which of the Cs oxides is formed upon O_2 exposure,²⁹ but the idea of Clark³⁰ that the optimum thickness should be about one monolayer of Cs_{2+x}O , $x > 0$, i.e., $x = 1$, is in agreement with our observation. Also Burt and Heine³¹ prove that the maximum reduction in phototreshold goes along with the formation of Cs_{11}O_4 , which is in the same direction. Electrons originating from the L -point valley are significantly less scattered in the Cs-O layer, which they traverse with a higher kinetic energy. Though in luminescence measurements these cannot be identified,¹⁰ they are clearly evident in our spectra (cf. Fig. 4).

B. PEA GaAs

As already mentioned there is a variety of possible PEA surfaces, each with a different phototreshold ϕ and a different ESP spectrum. Experimentally, we use the onset of photocurrent with cesiation at a chosen photon energy as a monitor in producing different PEA surfaces. Two examples are shown in Fig. 5. It is difficult to

get a quantitative understanding of the ESP, which is in general larger than that found with a NEA surface, as there are now many competing effects. In contrast to the NEA case, where the escape depth of the electrons is limited by the diffusion length of about 10^4 \AA ,¹² the size of the escape region is now given by the hot scattering length of less than 100 \AA ,¹² unless emission of L -electrons dominates. Their diffusion length is again larger ($\sim 500 \text{ \AA}$), so that escape cone effects play a minor role in that case.

In going away from the Γ point the twofold degenerate valence band splits into a heavy and a light hole band. The short escape depth enhances emission along the $\langle 110 \rangle$ direction, as only elec-

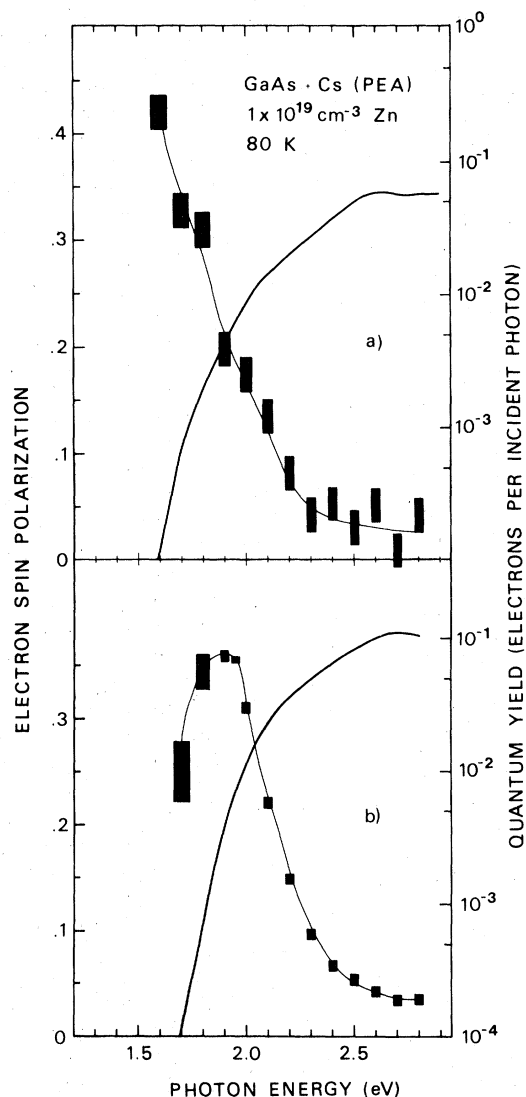


FIG. 5. Electron spin polarization and yield curve as in Fig. 4 for two different PEA GaAs cases at 80 K: (a) $\phi = 1.59$ eV, (b) $\phi = 1.7$ eV. See text also.

trons with sufficient momentum normal to the surface ($p_z^2/2m > \chi$, χ : electron affinity) can leave the crystal. Pierce *et al.*⁷ showed that due to the different escape cones for excitations from the heavy and light hole bands, P is weighted in favor of the heavy hole band, resulting in an initial polarization between 0.5 and 1.0; in particular $P_i = 0.77$ for $\chi = 68$ meV which corresponds to $\phi = 1.6$ eV of Fig. 5(a) in which we find $P_{\max}(\phi) = 0.43$. We have never observed $P > 0.50$ in the some 50 different spectra obtained from six crystals with different surface treatments. But if we assume the same bulk depolarization mechanism to be valid as in the NEA case, for which the theoretical initial polarization P_i is reduced by a factor of $0.5/0.3 = 1.67$ to the luminescence value P_L , we can understand the low threshold value. This assumption is supported by the observation that P_L remains constant up to $h\nu = 1.75$ eV,¹⁰ and that the spin relaxation and hot electron scattering times are of the same order of 10^{-11} sec.^{10,12}

When the threshold is raised by a further 0.1 eV to $\phi = 1.7$ eV [cf. Figs. 5(b) and 1(a)], the most highly polarized part of the ESP spectrum is cut off, and its shape is now determined by the emission of electrons from the L -point valley and resembles the NEA curve of Fig. 4(b) in general form. The maximum P at 0.35 is found around 1.95 eV. The decreasing trend at $h\nu < 1.8$ eV is due to Γ -valley electrons. A comparison of Figs. 5(a) and 5(b) shows that the low P value evident in Fig. 5(b) at 1.7 eV is masked in Fig. 5(a) by the inclusion of threshold electrons with higher polarization; this is a consequence of the integral type of measurement. The L -point polarization is suppressed in Fig. 5(a) due to the onset of negatively polarized electrons from the split-off part of the valence band at $h\nu = E_G + \Delta + \chi = 1.52 + 0.34 + 0.1 = 1.96$ eV. In Fig. 5(b) with $\chi \approx 0.2$ eV this onset occurs at $h\nu \approx 2.1$ eV and accounts for the decrease of P towards higher photon energies. Though it seems from the temperature dependence in Fig. 4 (cf. Sec. IV A) as if the intervally scattering from Γ to L is less depolarizing than the thermalization within the Γ valley, it is difficult to understand the 0.35 value quantitatively, as it is not known what proportion of negatively polarized electrons is actually participating. An energy selective measurement of the ESP would yield more information.

V. GaAs AS SOURCE OF SPIN POLARIZED ELECTRONS

Figure 4 clearly indicates that the use of NEA GaAs(110) as a source of polarized electrons, as originally proposed,⁷ is limited by the low maximum P . In this respect PEA surfaces are more prom-

ising, especially as the loss in Y can be easily compensated for by using an intense lamp. Luckily the high P at $h\nu = 1.96$ eV [cf. Fig. 5(b)] coincides with the resonance frequency of a He-Ne laser. Though such a PEA surface with $\phi = 1.7$ eV can be created by a moderate cesiation, monitored by observing the onset of photocurrent at this ϕ , it is found in practice that such a highly stable PEA is obtained by "aging" a NEA surface for about one day, followed if necessary by a slight recesiation. In such a manner high currents with $P = 0.35$ can be drawn from a cathode which retains its properties for days.

Preliminary results were obtained for GaAs crystals with a higher doping (5×10^{19} cm⁻³ Zn), as the luminescence results of Fishman and Lampel¹⁰ and Ekimov and Safarov³² from such crystals indicate a higher bulk polarization P_L . Generally we find the same kind of behavior as presented in Figs. 4 and 5, but without a significant increase in P . Practical difficulties also arise, as these higher doped samples do not cleave properly, but rather break with a step structure on the sometimes off-perpendicular surface. Samples with the lower doping are therefore preferred.

One major advantage of the GaAs source is the ease with which the spin-polarization vector may be reversed, without changing the electron optical properties. This is achieved by rotating the quarter wave plate through 90° , thereby changing the helicity of the light from σ_+ to σ_- . This is illustrated in Fig. 6.

The available beam current and the focal properties of the lens system are measured by replacing the target in the scattering chamber (cf. Fig. 3) by a stainless-steel screen with a fluorescent coating, maintained at a potential of 1.4 kV relative to cathode. To prevent the accelerating field from influencing the lens properties, four grids in front of the screen are maintained at the potential of the last lens element. These grids also serve to return secondary electrons to the screen. A retarding voltage on the center two grids enables an energy analysis of the spin-polarized electrons. The quality of the beam shape is shown by the fluorescent pattern on the screen observed through a view port.

It is found that a well defined spot of submillimeter diameter is obtained for a range of final kinetic energies of 30–400 eV. Problems encountered in focusing the beam below 30 eV are attributed to the absence of magnetic shielding in the present apparatus which is designed for scattering measurements in the 30–150 eV range. The beam current I_s on the screen is shown as a function of final kinetic energy in Fig. 7. The current varies only slightly over the range 70–240 eV with an

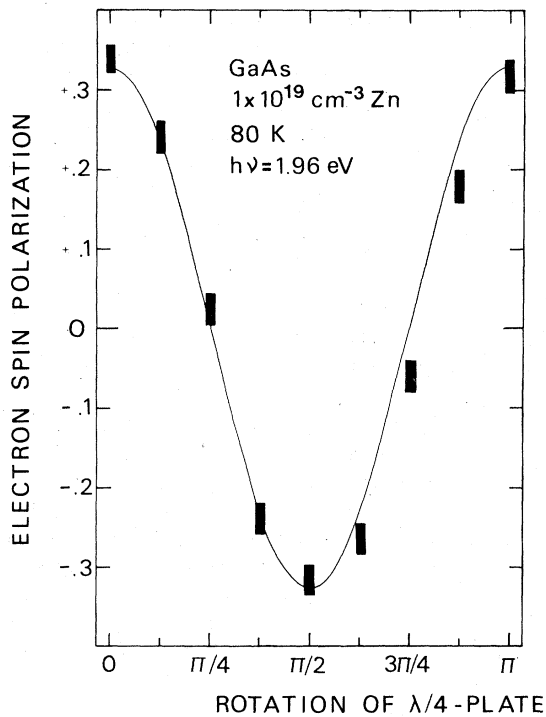


FIG. 6. Reversal of spin polarization by rotating the quarter wave plate through 90° . The solid line represents a sine curve.

average value of $1.5 \mu\text{A}$. The total current emitted from the cathode I_c is $10 \mu\text{A}$. Thus 15% of the emission current is measured on the final screen. This represents a lower limit to the beam current, since the four grid system has a total transparency

of less than 20%. Using the grids and screen together as a collector at L_1 potential (cf. Fig. 3) a current of $4 \mu\text{A}$ was measured.

Also shown in Fig. 7 is the ratio of voltages V_1 and V_2 applied to L_1 and L_2 , respectively, at a fixed V_3 , required to maximize the current at the collector, while keeping position and size of the final image independent of beam energy. The linearity for an electron energy $E > 100 \text{ V}$ facilitates the automatic recording of energy spectra.

Measurement of the energy distribution of the electrons at different primary energies shows a Gaussian with a half width at full maximum of typically 400 meV . This value is given by the resolution of the retarding-grid-type analyzer.³³ The true width is of the order of 0.2 eV .¹²

VI. SUMMARY

We have presented a simple design for a source of spin-polarized electrons using photoemission from GaAs(110). A polarized beam of $4 \mu\text{A}$ with $P = 0.35$ is well focused in the kinetic energy range of $30\text{--}400 \text{ eV}$. In contrast to earlier suggestions we do not use the electrons emitted at the Γ point, but those which have thermalized into the L -point valley. Our source combines all the necessary conditions for low-energy electron experiments with the advantage of an easy and quick spin reversal.³⁴ In high-energy physics a similar GaAs source has recently delivered³⁵ the necessary high accuracy to detect parity nonconservation in the electromagnetic interaction.

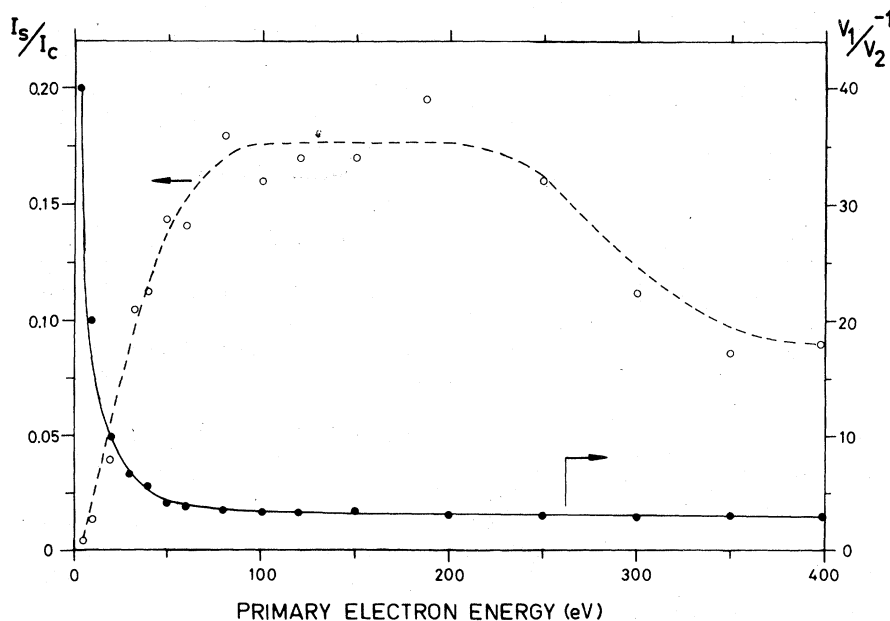


FIG. 7. Ratio of beam current measured at the screen, I_s , to the totally emitted current at the cathode, I_c (left ordinate, open dots) and ratio of voltages V_1/V_2^{-1} applied at L_1 and L_2 , respectively, with $V_3 = 50 \text{ V}$ (right ordinate, full dots) as function of primary electron energy in eV.

ACKNOWLEDGMENTS

Thanks are due to H. C. Siegmann for his encouragement during all stages of the experiment. We thank D. T. Pierce, Natl. Bur. Stand., Gaithersburg, for valuable comments. Our warm thanks

go to the workshop at the Laboratorium für Festkörperphysik for their able and kind help in building the apparatus. One of us (D. M. C.) thanks the ETH for support and hospitality as an academic guest. We acknowledge support by the Swiss National Science Foundation.

*Permanent address; Department of Physics, University of Edinburgh, United Kingdom.

- ¹A general review on the present status of spin-polarized electron physics is given by Kessler (Ref. 2). For the special aspects of solid-state physics, see Refs. 3–5.
- ²J. Kessler, in *Polarized Electrons* (Springer-Verlag, Berlin, Heidelberg, 1976).
- ³H. C. Siegmann, *Phys. Rep.* **17**, 39 (1975).
- ⁴M. Kalisvaart, M. R. O' Neill, T. W. Riddle, F. B. Dunning, and G. K. Walters, *Phys. Rev. B* **17**, 1570 (1978).
- ⁵E. Kisker, G. Baum, A. H. Mahan, W. Raith, and B. Reihl, *Phys. Rev. B* **18**, 2256 (1978).
- ⁶E. Garwin, D. T. Pierce, and H. C. Siegmann, *Helv. Phys. Acta* **47**, 343 (1974).
- ⁷D. T. Pierce, F. Meier, and P. Zürcher, *Appl. Phys. Lett.* **26**, 670 (1975); D. T. Pierce and F. Meier, *Phys. Rev. B* **13**, 5484 (1976).
- ⁸M. Erbudak and B. Reihl, *Appl. Phys. Lett.* **33**, 584 (1978).
- ⁹R. R. Parsons, *Phys. Rev. Lett.* **23**, 1152 (1969).
- ¹⁰G. Fishman and G. Lampel, *Phys. Rev. B* **16**, 820 (1977).
- ¹¹W. E. Spicer, *Appl. Phys.* **12**, 115 (1977).
- ¹²L. W. James and J. L. Moll, *Phys. Rev.* **183**, 740 (1969).
- ¹³D. E. Aspnes, *Phys. Rev. B* **14**, 5331 (1976).
- ¹⁴S. A. E. S. Getters, 20151 Milan, Italy; No. 12T14 + 14.
- ¹⁵Polaroid Corp., Cambridge, Mass.
- ¹⁶Bernhard Halle Nachfl., 1 Berlin 41, West Germany.
- ¹⁷E. M. Purcell, *Phys. Rev.* **54**, 818 (1938).
- ¹⁸M. V. Kurepa, M. D. Tasic, and J. M. Kurepa, *J. Phys. E* **7**, 940 (1974).
- ¹⁹A. B. El-Kareh and J. C. J. El-Kareh, in *Electron Beams, Lenses and Optics* (Academic, New York, 1970).
- ²⁰Wacker-Chemitronic, 8263 Burghausen, West Germany.
- ²¹A. J. van Bommel and J. E. Grombeen, *Surf. Sci.* **45**, 308 (1974).
- ²²For the theoretical background of Mott scattering, see Ref. 2. The experimental procedures are described in Refs. 3–5.
- ²³Siemens, Model GO3N20/200 A.
- ²⁴Métaux Précieux SA, 2000 Neuchâtel, Switzerland.
- ²⁵V. K. Mathur and S. Rogers, *Appl. Phys. Lett.* **31**, 765 (1977).
- ²⁶D. E. Eastman and J. L. Freeouf, *Phys. Rev. Lett.* **33**, 1601 (1974); A. Huijser, J. van Laar, and T. L. van Rooy, *Surf. Sci.* **62**, 472 (1977).
- ²⁷G. L. Bir, A. G. Aronov, and G. E. Pikus, *Sov. Phys. JETP* **42**, 705 (1976).
- ²⁸D. M. Campbell, H. M. Brash, and P. S. Farago, *Phys. Lett. A* **36**, 449 (1971).
- ²⁹P. E. Gregory, P. Chye, H. Sunami, and W. E. Spicer, *J. Appl. Phys.* **46**, 3525 (1975).
- ³⁰M. G. Clark, *J. Phys. D* **8**, 535 (1975).
- ³¹M. G. Burt and V. Heine, *J. Phys. C* **11**, 961 (1978).
- ³²A. I. Ekimov and V. I. Safarov, *JETP Lett.* **13**, 495 (1971).
- ³³J. A. Simpson, *Rev. Sci. Instrum.* **32**, 1283 (1961).
- ³⁴For detailed comparison of *all* sources suitable for low-energy electron scattering, the reader is referred to Ref. 5. See also G. Baum, E. Kisker, A. H. Mahan, W. Raith, and B. Reihl, *Appl. Phys.* **14**, 149 (1977).
- ³⁵C. M. Prescott *et al.*, *Phys. Lett. B* **77**, 347 (1978); *Physics Today* **31**, 17 (1978).